ChemComm

COMMUNICATION

View Article Online
View Journal | View Issue

Published on 04 February 2015. Downloaded by University of California - San Diego on 10/03/2015 18:25:55.

Cite this: *Chem. Commun.*, 2015, 51, 4402

Received 8th December 2014,
Accepted 4th February 2015

DOI: 10.1039/c4cc09584g

www.rsc.org/chemcomm

All-atom lipid bilayer self-assembly with the AMBER and CHARMM lipid force fields†

Åge A. Skjevik,[ab] Benjamin D. Madej,[ac] Callum J. Dickson,[d] Knut Teigen,[b] Ross C. Walker*[ac] and Ian R. Gould*[d]

This communication reports the first example of spontaneous lipid bilayer formation in unbiased all-atom molecular dynamics (MD) simulations. Using two different lipid force fields we show simulations started from random mixtures of lipids and water in which four different types of phospholipids self-assemble into organized bilayers in under 1 microsecond.

The study of lipid membranes and protein–membrane interactions with MD simulations is important for several reasons. Membranes and their protein constituents are almost omnipresent in the body and have many essential biological roles, yet their inherent fluidity often complicates experimental studies. This is probably best reflected by the low number of resolved membrane bound protein structures when compared to the total number of experimentally determined protein structures. Considering that membrane proteins constitute the largest group of present-day drug targets, protein–membrane simulation studies are also highly relevant from a drug development perspective. The development of high-fidelity force fields for the simulation of lipid membranes is thus a topic of broad interest.

Phospholipids placed in an aqueous environment will spontaneously aggregate in order to minimize thermodynamically unfavourable contacts between their long hydrophobic acyl chains and water or other polar molecules. In that regard, a lamellar bilayer, the essential structural basis of biological membranes, is often the most energetically favourable molecular arrangement and the configuration adopted by phospholipids under physiological conditions.

Molecular dynamics (MD) simulations have previously shown self-assembly of phospholipids randomly distributed in water into bilayer[1–5] and vesicle[5–7] structures, as well as lipid bilayer formation around proteins,[8,9] peptides[2,8] and DNA.[10] However, all the lipids in these simulations – and in some cases other molecules as well – were modelled using either united atom[1–4,6] or coarse-grained force fields.[5,7–10] In united atom models the aliphatic hydrogens are implicitly represented and considered part of a bigger unit that also contains the carbon atom to which they are bonded. The molecular resolution in coarse-grained representations is even lower. Typically 5 or more atoms are grouped together into a single interaction particle, the principal idea being to provide an approximation that reduces the degrees of freedom and so maximizes simulation speed and provides access to longer timescales.

The self-assembly simulations in the present work employ all-atom representations using the recently published AMBER Lipid14 force field[11] as well as the CHARMM36 force field for lipids (C36).[12] Lipid14 is the first modular lipid force field, and is compatible with the other AMBER parameter sets for proteins, nucleic acids, carbohydrates and small molecules. The modular parameterization strategy allows for any combination of different phospholipid head groups and tails to create custom lipid molecules. At the time of writing there are parameters developed for phosphatidylcholine (PC) and phosphatidylethanolamine (PE) head groups and lauroyl (LA), myristoyl (MY), palmitoyl (PA) and oleoyl (OL) tails. This provides for 32 possible lipid types.

For this initial work four phospholipid types were chosen for self-assembly simulations, all of them commonly found in biological membranes; dipalmitoyl-phosphatidylcholine (DPPC), palmitoyl-oleoyl-phosphatidylcholine (POPC), dioleoyl-phosphatidylcholine (DOPC) and palmitoyl-oleoyl-phosphatidylethanolamine (POPE). This set includes two different head groups (PC and PE) as well as tails with varying degrees of unsaturation (a total of 0, 1 or 2 aliphatic double bonds). Additionally the experimental data available for these four phospholipids are the most comprehensive.

[a] *San Diego Supercomputer Center, University of California San Diego, 9500 Gilman Drive MC0505, La Jolla, California, 92093-0505, USA. E-mail: ross@rosswalker.co.uk*
[b] *Department of Biomedicine, University of Bergen, N-5009 Bergen, Norway*
[c] *Department of Chemistry and Biochemistry, University of California San Diego, 9500 Gilman Drive MC0505, La Jolla, California, 92093-0505, USA*
[d] *Department of Chemistry and Institute of Chemical Biology, Imperial College London, South Kensington, SW7 2AZ, UK. E-mail: i.gould@imperial.ac.uk*

† Electronic supplementary information (ESI) available: Videos from self-assembly simulations (accompanying captions provided in the PDF file), a detailed methods section, simulation system details, additional properties calculated for the self-assembled bilayers, figures showing the PC and PE head group charges in Lipid14 and C36 as well as snapshots from C36 DPPC self-assembly are included. See DOI: 10.1039/c4cc09584g

This journal is © The Royal Society of Chemistry 2015

Published on 04 February 2015. Downloaded by University of California - San Diego on 10/03/2015 18:25:55.

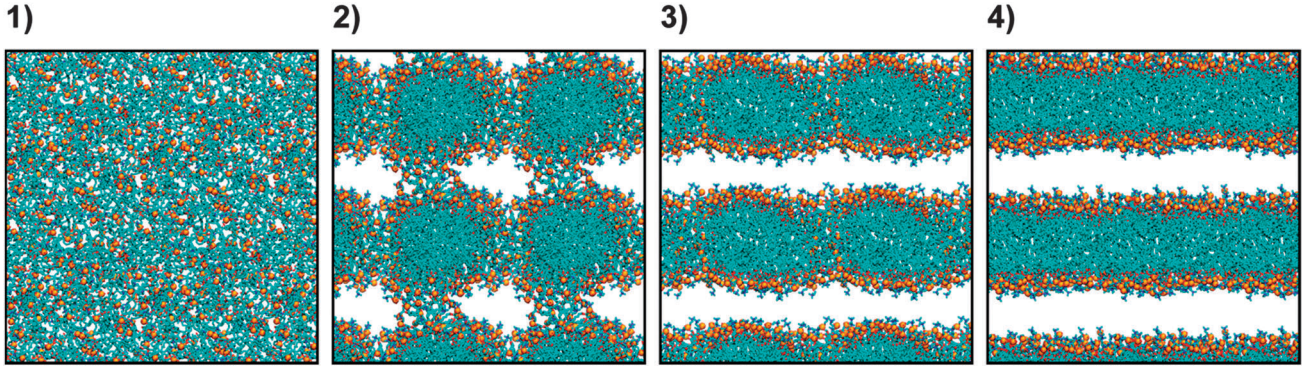

Fig. 1 General mechanism of the all-atom bilayer self-assembly. Representative snapshots from one of the DOPC simulations illustrate four characteristic stages in the self-assembly process (see main text for details). The phospholipids are represented as stick models, with the head group phosphorus atoms highlighted as orange spheres. For clarity, water, ions and hydrogens are not shown. Note that each snapshot not only includes the primary simulation box, but also portions of surrounding periodic images.

All simulations were run using the GPU accelerated version of AMBER 14,[13–16] with the SPFP precision model.[17] Simulation details are given in the methods section of the ESI,† and specifics for each of the four simulation systems, such as number of lipids, water to lipid ratio, simulation length and ion concentration, can be found in Table S1 (ESI†). Three repeats (1 μs each) were run for each lipid type using both parameter sets, amounting to 24 μs of aggregate simulation time.

In all of the simulations, the lipids self-assembled into bilayers *via* the same general pathway (see also Videos S1–S4, ESI†), the stages of which resemble intermediate states reported in self-assembly studies utilizing united atom models.[1,3,4] Fig. 1 provides representative snapshots from one of the simulations illustrating these individual stages, which are described below. The starting structures for the self-assembly simulations consisted of lipids randomly distributed in aqueous surroundings (snapshot 1). Initially the non-polar aliphatic lipid tails quickly congregate to escape the polar aqueous environment. Within 80 ns, a main aggregate of lipids forms with the lipid tails oriented towards the centre, reminiscent of the cross-section of a micelle (snapshot 2). Some of the lipids though, referred to as "lipid bridges" by de Vries *et al.*,[1] reside between and connect the lipid assembly and its periodic images. As the simulations progress, the lipid bridges along one dimension incorporate into the lipid assembly, which transforms into a lamellar bilayer-like configuration penetrated by a water pore lined with several lipid head groups (snapshot 3). Once the lipid head groups leave the non-polar region of the bilayer-like structure and water is excluded from the hydrophobic interior, a fully assembled bilayer is formed (snapshot 4). In some of the simulations the pore disappears before all the bridge lipids are incorporated into the bilayer structure, and for the fastest self-assemblies the different stages can overlap and be difficult to distinguish. All the bilayer formation times are listed in Table 1. These vary greatly, even in repeat simulations on the same phospholipid system, as has also been the case in other self-assembly studies.[2–4] Considering the Lipid14 results in isolation, POPE is an exception in this

Table 1 Characteristics of the self-assembled Lipid14 and C36 bilayers and comparison with experiment

		Bilayer formation time (ns)		Number of lipids per leaflet		Area per lipid[b] (Å^2)			Isothermal compressibility modulus K_A[b] (mN m^{-1})			Lateral diffusion coefficient[c] (10^{-8} cm^2 s^{-1})		
Lipid	Sim. no.[a]	Lipid14	C36	Lipid14	C36	Lipid14	C36	Exp.	Lipid14	C36	Exp.	Lipid14	C36	Exp.
DOPC	1	150	135	66/62	61/67	69.3 ± 1.2	67.8 ± 1.2	67.4,[23] 72.5[28]	315.4	331.6	265,[31]	9.88	8.58	11.5,[21] 17[27]
	2	285	145	62/66	67/61	69.2 ± 1.1	67.8 ± 1.1		351.9	356.4	300,[20] 318[19]	7.89	6.67	
	3	720	160	63/65	65/63	69.0 ± 1.2	67.6 ± 1.1		288.7	348.3		7.63	8.10	
POPC	1	375	160	64/64	66/62	65.5 ± 1.2	63.8 ± 1.2	64.3,[24] 68.3[25]	308.5	275.9	180–330[18]	7.12	6.08	10.7[21]
	2	535	325	63/65	66/62	65.7 ± 1.3	63.7 ± 1.2		259.7	289.0		7.44	8.77	
	3	755	425	68/60	62/66	65.6 ± 1.3	63.8 ± 1.1		245.6	320.5		6.97	8.65	
POPE	1	70	95	62/66	61/67	56.0 ± 1.1	56.9 ± 1.1	56.6,[29] 59–60[30]	321.2	308.4	233[29]	3.94	6.52	5.2[22d]
	2	100	115	63/65	62/66	56.3 ± 1.1	56.5 ± 1.1		314.1	304.3		6.14	5.08	
	3	125	205	71/57	67/61	57.2 ± 1.3	56.9 ± 1.1		240.3	305.8		6.75	6.37	
DPPC	1	230	35	65/63	66/62	62.2 ± 1.4	57.1 ± 2.6	63.1,[24] 64.3[26]	212.2	57.3	231[28]	9.74	0.65	12.5,[33] 15.2[32]
	2	350	85	64/64	64/64	62.3 ± 1.3	53.7 ± 2.7		252.0	52.2		9.53	0.65	
	3	440	325	60/68	62/66	62.3 ± 1.4	55.4 ± 2.0		218.2	98.1		10.48	0.80	

[a] Simulation number; both the Lipid14 and C36 repeats for each lipid type have been sorted in ascending order based on bilayer formation time. [b] Calculated from the interval from 50 ns after bilayer was fully formed until 1 μs of total simulation time. Due to an initial bilayer equilibration phase, the properties were calculated from the last 400 ns for the last Lipid14 DPPC repeat listed. [c] Calculated from the last 100 ns of each self-assembly simulation. [d] Cell culture membrane containing 78% POPE at 305 K.

Published on 04 February 2015. Downloaded by University of California - San Diego on 10/03/2015 18:25:55.

respect and our simulations suggest that the POPE lipids self-assemble faster than their phosphatidylcholine counterpart and faster than DOPC and DPPC with Lipid14. This may in part be related to the nature of the head groups. Compared to PC, the PE head group is smaller and less bulky, with hydrogens substituted on the terminal amine nitrogen instead of methyl groups. Another trend in Table 1 is that the C36 PC lipids seem to self-assemble faster than their Lipid14 equivalents, whereas the POPE bilayer formation times are quite similar when comparing the two force fields. The head group charges might provide part of the explanation. There are notable charge differences in PC between Lipid14 and C36 (Fig. S1, ESI†), especially in the choline portion, and the individual C36 point charges are often greater than the corresponding Lipid14 charges. Conversely, the differences are less pronounced in the PE head group (Fig. S2, ESI†). Also, the charge deviations between Lipid14 and C36 in the phosphate group (and glycerol region) are approximately the same for PE as for PC.

When the self-assembled bilayers had relaxed and equilibrated, the simulations were extended for several hundred additional nanoseconds, throughout which all the bilayer structures, apart from the C36 DPPC lipid systems, remained stable. The last portion of each simulation, with a starting point 50 ns after a bilayer was observed to have formed, was subsequently used for calculating average structural bilayer properties (for details regarding the analyses, consult the ESI†). Given in Table 1 are areas per lipid, isothermal compressibility moduli (K_A) and lateral diffusion coefficients (D) calculated for the self-assembled Lipid14 and C36 bilayers, along with experimental data.[18–33] Additional analysis is provided in the ESI,† including volumes per lipid and bilayer (D_{HH}) and Luzzati (D_B) thicknesses (Table S2, ESI†). The properties of the self-assembled Lipid14 and C36 (except DPPC) bilayers are in reasonable agreement with experimental values, indicating that the bilayer structures satisfactorily reproduce those determined experimentally. On the other hand, the C36 DPPC bilayer properties deviate significantly from the experimental data. The reason is that the DPPC lipids, in all three C36 repeats, eventually adopt a highly ordered configuration in which the tails from opposite leaflets overlap completely with each other in parts of the bilayer (Fig. S3, ESI†).

The computed Lipid14 areas per lipid are very close to the averages reported in the original validation of the Lipid14 force field,[11] as is also the case for the volumes per lipid and thicknesses. Interestingly the Lipid14 isothermal compressibility moduli and lateral diffusion coefficients in Table 1 generally show better agreement with experiment relative to the Lipid14 validation results.[11] Such bilayer characteristics might affect the interplay between the phospholipids and other molecules. Our results suggest that self-assembly may be a more effective strategy than starting simulations from preformed bilayers in some cases, particularly when the aim is to introduce proteins or other interaction partners into the membrane environment.

In most of the simulations, the lipids partitioned asymmetrically between the two leaflets of the assembled bilayer (Table 1). However, the average bilayer properties calculated for all four Lipid14 lipid types compare well with experiment and show close similarity to the corresponding Lipid14 validation results obtained from simulations of symmetric bilayers, indicating that the observed leaflet asymmetries are well tolerated. Varying degrees of asymmetry have also been reported for spontaneously aggregated united atom bilayers,[1–3] and to similar extents as observed here in self-assembly simulations of united atom 1 : 1 DOPC/DOPE mixtures.[1]

To summarize, beginning from random configurations, the four phospholipid types simulated aggregate into stable bilayers showing reasonable structural properties during the course of the simulations. It is our belief that this is the first time bilayer self-assembly has been demonstrated with all-atom MD simulations. In addition, bilayer formation occurred more rapidly than might have been expected from the timescales observed in united atom and coarse-grained studies demonstrating that lipid self-assembly with all atoms explicitly treated is more feasible than previously envisioned.

As well as serving as further validation of the AMBER Lipid14 force field, these simulations pave the way for several applications of biochemical interest. In contrast to ''manual'' insertion of proteins into premade bilayers prior to simulation, self-assembly of united atom or coarse-grained phospholipids around peptides and proteins has been performed as an unbiased approach to obtain protein–membrane complexes and for predicting the position of proteins or peptides in bilayers.[2,8,9] Nevertheless, full atomic resolution might be required for accurately modelling the interactions between the membrane proteins and the surrounding self-assembled lipid environment. Lipid14 offers the possibility for simulation of lipids together with other types of all-atom molecules, including peptides and proteins, and our self-assembly simulations indicate that these applications should be feasible at the all-atom level of detail. A more comprehensive study of self-assembly using several all-atom force fields, a broader selection of lipid types as well as mixtures of proteins with lipids will form the basis of future work. It is also worth mentioning that the formation of a small vesicle-like structure composed of phospholipids has already been demonstrated in a united atom simulation.[6] In light of the current results, it is not unreasonable to expect that similar complex lipid structure self-assembly might be possible with the latest generation all-atom models.

We are very grateful to Dr Hannes Loeffler of the Science and Technology Facilities Council, UK, for writing and maintaining the modified PTRAJ/CPPTRAJ routines that were used in this work. ÅAS and K.T. acknowledge the support of the Strategic Programme for International Research and Education (SPIRE) and the Meltzer Foundation. IRG and CJD thank the Institute of Chemical Biology, UK Biotechnology and Biological Sciences Research Council (BBSRC) and GlaxoSmithKline for the award of a studentship to CJD. IRG would also like to acknowledge funding from the EU in the form of the project ''HeCaToS – Hepatic and Cardiac Toxicity Systems modeling'' FP7-HEALTH-2013-INNOVATION-1 (Project number 602156). BDM would like to acknowledge funding for this work provided by the NIH Molecular Biophysics Training Grant (T32 GM008326) and the NVIDIA Graduate Fellowship Program. RCW and ÅAS acknowledge funding through NSF SI2-SSE grant (NSF-1148276) to RCW. RCW also acknowledges funding through fellowships from Intel Corporation and NVIDIA, Inc.

 This journal is © The Royal Society of Chemistry 2015

Published on 04 February 2015. Downloaded by University of California - San Diego on 10/03/2015 18:25:55.

Notes and references

1 A. H. de Vries, A. E. Mark and S. J. Marrink, *J. Phys. Chem. B*, 2004, **108**, 2454–2463.
2 S. Esteban-Martín and J. Salgado, *Biophys. J.*, 2007, **92**, 903–912.
3 S. J. Marrink, E. Lindahl, O. Edholm and A. E. Mark, *J. Am. Chem. Soc.*, 2001, **123**, 8638–8639.
4 D. Poger, W. F. van Gunsteren and A. E. Mark, *J. Comput. Chem.*, 2010, **31**, 1117–1125.
5 W. Shinoda, R. DeVane and M. L. Klein, *J. Phys. Chem. B*, 2010, **114**, 6836–6849.
6 A. H. de Vries, A. E. Mark and S. J. Marrink, *J. Am. Chem. Soc.*, 2004, **126**, 4488–4489.
7 S. J. Marrink and A. E. Mark, *J. Am. Chem. Soc.*, 2003, **125**, 15233–15242.
8 P. J. Bond, J. Holyoake, A. Ivetac, S. Khalid and M. S. P. Sansom, *J. Struct. Biol.*, 2007, **157**, 593–605.
9 K. A. Scott, P. J. Bond, A. Ivetac, A. P. Chetwynd, S. Khalid and M. S. P. Sansom, *Structure*, 2008, **16**, 621–630.
10 S. Khalid, P. J. Bond, J. Holyoake, R. W. Hawtin and M. S. P. Sansom, *J. R. Soc., Interface*, 2008, **5**, S241–S250.
11 C. J. Dickson, B. D. Madej, Å. A. Skjevik, R. M. Betz, K. Teigen, I. R. Gould and R. C. Walker, *J. Chem. Theory Comput.*, 2014, **10**, 865–879.
12 J. B. Klauda, R. M. Venable, J. A. Freites, J. W. O'Connor, D. J. Tobias, C. Mondragon-Ramirez, I. Vorobyov, A. D. MacKerell, Jr. and R. W. Pastor, *J. Phys. Chem. B*, 2010, **114**, 7830–7843.
13 D. A. Case, V. Babin, J. T. Berryman, R. M. Betz, Q. Cai, D. S. Cerutti, T. E. Cheatham, III, T. A. Darden, R. E. Duke, H. Gohlke, A. W. Götz, S. Gusarov, N. Homeyer, P. Janowski, J. Kaus, I. Kolossváry, A. Kovalenko, T. S. Lee, S. Le Grand, T. Luchko, R. Luo, B. D. Madej, K. M. Merz, F. Paesani, D. R. Roe, A. Roitberg, C. Sagui, R. Salomon-Ferrer, G. Seabra, C. Simmerling, W. Smith, J. Swails, R. C. Walker, J. Wang, R. M. Wolf, X. Wu and P. A. Kollman, *AMBER 14*, University of California, San Francisco, 2014.
14 A. W. Götz, M. J. Williamson, D. Xu, D. Poole, S. Le Grand and R. C. Walker, *J. Chem. Theory Comput.*, 2012, **8**, 1542–1555.
15 R. Salomon-Ferrer, D. A. Case and R. C. Walker, *Wiley Interdiscip. Rev.: Comput. Mol. Sci.*, 2013, **3**, 198–210.
16 R. Salomon-Ferrer, A. W. Götz, D. Poole, S. Le Grand and R. C. Walker, *J. Chem. Theory Comput.*, 2013, **9**, 3878–3888.
17 S. Le Grand, A. W. Götz and R. C. Walker, *Comput. Phys. Commun.*, 2013, **184**, 374–380.
18 H. Binder and K. Gawrisch, *J. Phys. Chem. B*, 2001, **105**, 12378–12390.
19 E. Evans, personal communication – DOPC isothermal compressibility modulus from X-ray data at 293 K, 2014.
20 E. Evans, W. Rawicz and B. A. Smith, *Faraday Discuss.*, 2013, **161**, 591–611.
21 A. Filippov, G. Orädd and G. Lindblom, *Langmuir*, 2003, **19**, 6397–6400.
22 A. J. Jin, M. Edidin, R. Nossal and N. L. Gershfeld, *Biochemistry*, 1999, **38**, 13275–13278.
23 N. Kučerka, J. F. Nagle, J. N. Sachs, S. E. Feller, J. Pencer, A. Jackson and J. Katsaras, *Biophys. J.*, 2008, **95**, 2356–2367.
24 N. Kučerka, M.-P. Nieh and J. Katsaras, *Biochim. Biophys. Acta*, 2011, **1808**, 2761–2771.
25 N. Kučerka, S. Tristram-Nagle and J. F. Nagle, *J. Membr. Biol.*, 2005, **208**, 193–202.
26 N. Kučerka, S. Tristram-Nagle and J. F. Nagle, *Biophys. J.*, 2006, **90**, L83–L85.
27 J. Kuśba, L. Li, I. Gryczynski, G. Piszczek, M. Johnson and J. R. Lakowicz, *Biophys. J.*, 2002, **82**, 1358–1372.
28 J. F. Nagle and S. Tristram-Nagle, *Biochim. Biophys. Acta*, 2000, **1469**, 159–195.
29 R. P. Rand and V. A. Parsegian, *Biochim. Biophys. Acta*, 1989, **988**, 351–376.
30 M. Rappolt, A. Hickel, F. Bringezu and K. Lohner, *Biophys. J.*, 2003, **84**, 3111–3122.
31 W. Rawicz, K. C. Olbrich, T. McIntosh, D. Needham and E. Evans, *Biophys. J.*, 2000, **79**, 328–339.
32 H. A. Scheidt, D. Huster and K. Gawrisch, *Biophys. J.*, 2005, **89**, 2504–2512.
33 W. L. C. Vaz, R. M. Clegg and D. Hallmann, *Biochemistry*, 1985, **24**, 781–786.